doi:10.1246/cl.2010.1242

Published on the web October 30, 2010

Phase Transition and Thermal Behavior Change of Low Silica X Zeolite at [Al] = 90

Mana Yasui-Hiraiwa,[1] Teruhisa Hongo,*[2] Hiroko Hayashi,[1] Tetsuo Takaishi,[3] Shinichi Nataka,[4] and Atsushi Yamazaki[1]
[1]*Department of Resources and Environmental Engineering, School of Creative Science and Engineering, Waseda University, 3-4-1 Okubo, Shinjuku-ku, Tokyo 169-8555*
[2]*Department of Materials and Life Science, Faculty of Science and Technology, Seikei University, 3-3-1 Kichijoji-Kitamachi, Musashino, Tokyo 180-8633*
[3]*Department of Materials Science, Toyohashi University of Technology, 1-1 Hibarigaoka, Tempaku-cho, Toyohashi, Aichi 441-8580*
[4]*Department of Materials Process Engineering and Applied Chemistry for Environments, Faculty of Engineering and Resource Science, Akita University, 1-1 Tegata Gakuen-machi, Akita 010-8502*

(Received August 19, 2010; CL-100717; E-mail: hongo@st.seikei.ac.jp)

Low silica X zeolite samples in the composition region of the number of Al atoms per unit cell ([Al]) between 84 and 96 were synthesized. X-ray diffraction and nuclear magnetic resonance analyses of the obtained samples verify the existence of the phase transition point and confirm the changes in the thermal behaviors of the samples at [Al] = 90.

Zeolites are microporous crystalline aluminosilicates in which the structural framework contains tetrahedral TO_4 units (T: Si or Al) linked together by oxygen sharing.[1] The general formula of zeolite is $M^{n+}[Si_xAl_yO_z]\cdot mH_2O$, where M^{n+} are extract-framework cations, $[Si_xAl_yO_z]$ is the zeolite framework, and mH_2O are sorbed water molecules.[2] Zeolites have been widely used in several industrial applications, for example, as catalysts in fluid cracking, sorbents in volatile organic removal, solid-state hydrogen storage media, and ion exchangers.[3–7] The presence and distribution of aluminum in zeolites markedly affect the degree of cation exchange and the strength of acidity in their hydrogen form.[8] The Si and Al ordering must follow Loewenstein's rule about the absence of Al–O–Al linkages.[9]

Faujasite (FAU)-type zeolites are commonly classified into the following two classes: X (low silica X: LSX) with a Si/Al ratio between 1 and 1.5 and Y with a Si/Al ratio above 1.5.[10] Dempsey et al. reported that FAU zeolite has three gaps of lattice constants and phase transitions as a function of the number of Al atoms per unit cell ([Al]) at 54, 66, and 78.[11] Later, Takaishi predicted another transition point at about [Al] = 90 from a theoretical consideration about the distribution changes of Al atoms in the FAU framework on the basis of previous experimental reports.[12] The secondary building unit (SBU) of FAU is a double six-membered ring (D6R),[13] which contains six or three Al atoms (abbreviated as D6R-6 and D6R-3, respectively). By connecting four D6Rs, five types of tertiary building unit (TBU) can be constructed. The unit cell of FAU zeolite is formed by four TBUs of the same type, resulting in five types of FAU zeolite, the phase boundaries of which exist at about [Al] = 54, 66, 78, and 90.[12] However, the experimental and crystal structure data of LSX zeolite in the composition region of $90 < [Al] < 96$ has been deficient.

In this study, LSX zeolite in the composition region of $84 < [Al] < 96$ was synthesized and examined in terms of the phase transition at about [Al] = 90. Moreover, the thermal stability and thermal behaviors of the LSX zeolite in the temperature range up to 1000 °C were investigated.

LSX zeolites were prepared by two methods. Na LSX zeolite samples in the composition region of $88 < [Al] < 96$ were prepared by a procedure similar to that described by Dempsey et al.[11] The Na LSX zeolite samples of about [Al] = 85 were prepared by a procedure similar to that described by Lechert and Kacirek.[14]

X-ray powder diffraction (XRD) analysis was performed using a Rigaku Rad-IX diffractometer with graphite monochromatized Cu Kα radiation (40 kV, 20 mA). Lattice constants were refined using the software of Rlc3. The diffraction angles of the XRD peaks were determined using standard silicon. High-temperature XRD (HT-XRD) data were obtained using a high-temperature unit attached to the former XRD system. Chemical analysis was carried out using an energy-dispersive analysis system (Link Co., Ltd. Qx 2000J) installed on a scanning electron microscope (SEM) (JEOL JSM5400). Thermal analyses were conducted with a Rigaku TAS-100 at a heating rate of 10 K min^{-1} in static air. ^{29}Si magic angle spinning nuclear magnetic resonance (MAS-NMR) spectra were recorded on a JEOL NMR400 spectrometer operating at a frequency of 79 MHz, and they were used to calculate the framework Si/Al ratio. All the spectra were recorded with a 5-mm double-bearing MAS probe at a spinning frequency of 5 kHz.

All of the obtained samples were identified as a single phase of LSX zeolite in the XRD patterns. Typical XRD patterns are shown in Figure 1. The sample of [Al] = 90 shows a weak (111) diffraction line and a poor peak separation of the other lines. This suggests that LSX zeolite samples with [Al] very close to 90 have a partial crystallographic disturbance. Figure 2 shows the lattice constants of the samples as cubic symmetry a_0 depends on their [Al]. The lattice constant gap at about [Al] = 90 is clearly observed, showing the existence of a phase transition boundary.

Figure 3 shows the theoretical (solid line) and experimental (dot) data for the number of Si(nAl) as a function of [Al] in the LSX zeolite framework, where the Si(nAl) denotes the central Si atom in the $Si(SiO)_{4-n}(AlO)_n$ unit. The theoretical data are lined according to a report published by Takaishi.[12] The report described the symmetry changes from $R3$ (or $\bar{R}$) to $Fd3$ at phase boundaries at [Al] = 90, which has been observed in the study of the ordered distribution of Al atoms in the FAU zeolite framework. Changes in the observed number of Si(nAl) per unit cell vs. [Al] show good correspondence with the theoretical trend. These results verify the existence of the phase transition point at about [Al] = 90 in LSX zeolite.

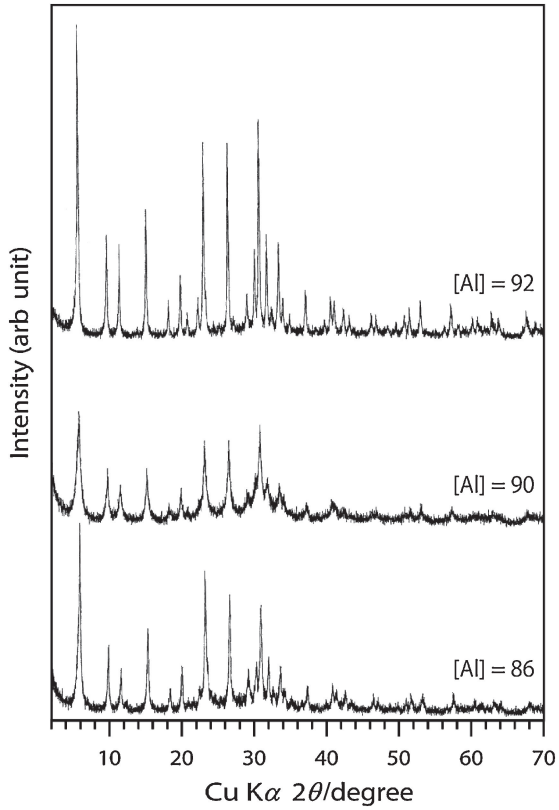

Figure 1. XRD patterns of synthesized sample of [Al] = 86, 90, and 92.

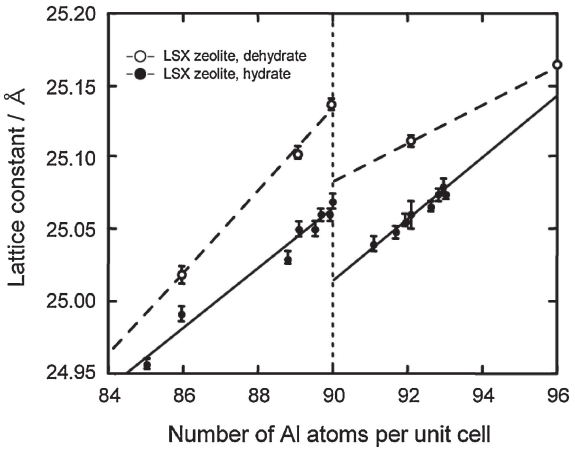

Figure 2. Lattice constants of obtained LSX samples as a function of [Al].

Figure 4 shows the DTA curves of the obtained LSX zeolites. The samples of [Al] $\leqq$ 90 have one exothermic peak at approximately 930 °C. In contrast, the sample of [Al] = 93 has two exothermic peaks at 818 and 918 °C. Considering the results of the HT-XRD measurements,[15] the zeolite structure of [Al] $\leqq$ 90 becomes amorphous at 900 °C after dehydration and recrystallizes to carnegieite (ICDD No. 11-0220) at approximately 930 °C. As for [Al] = 93, the zeolite structure becomes amorphous at 800 °C and recrystallizes to carnegieite at 818 °C. By further heating to 918 °C, carnegieite transforms to nepheline

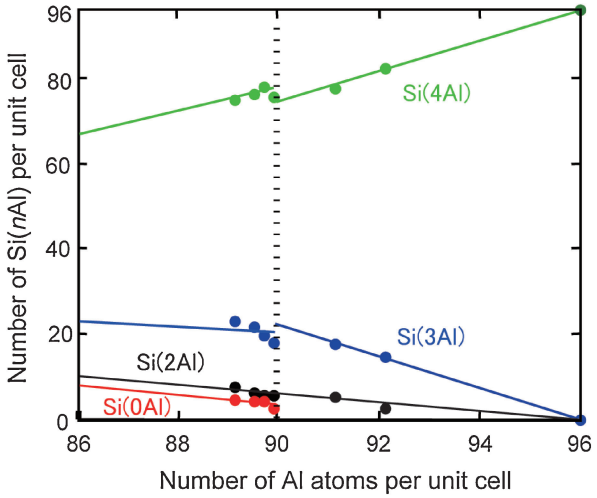

Figure 3. Number of Si(nAl) per unit cell as a function of [Al].

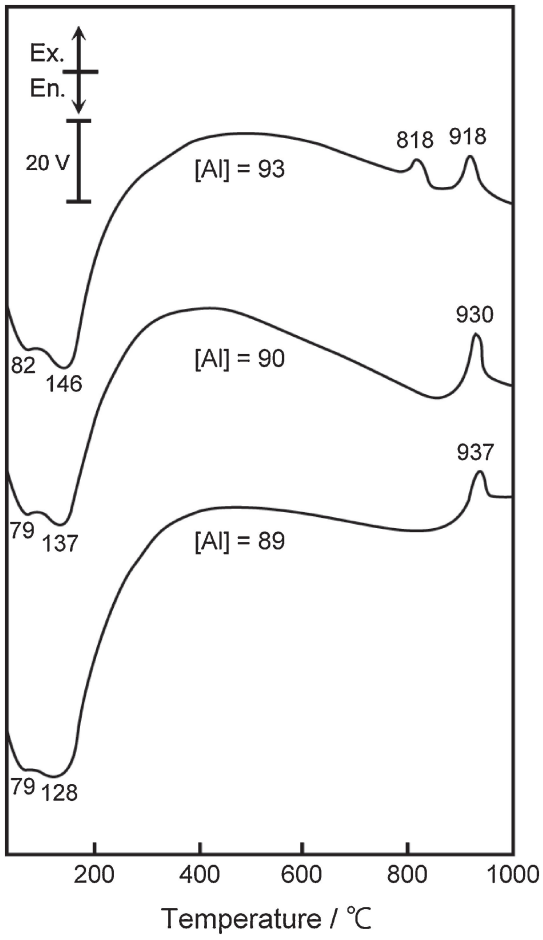

Figure 4. DTA curves of obtained LSX samples of [Al] = 89, 90, and 93.

(ICDD No. 35-0424). Therefore, the thermal behavior of LSX zeolite changes at the boundary of [Al] = 90. When [Al] exceeds 90, the thermal stability of the FAU zeolite structure

decreases, together with the generation of the carnegieite phase at low temperatures and that of the nepheline phase below 1000 °C. This is in agreement with a general trend indicating that the thermal stability of the zeolite structure decreases with increasing Al content.

In conclusion, LSX zeolites in the composition region of $84 < [Al] < 96$ were synthesized. The experimental results of the lattice constant gap and the trend of the number of Si(nAl) vs. [Al] verify the existence of the phase transition point at $[Al] = 90$ in LSX zeolite. The thermal behaviors of the samples also change at $[Al] = 90$: LSX zeolite of $[Al] > 90$ show a decrease in thermal stability and recrystallizes to carnegieite and nepheline phases at low temperatures compared with the LSX zeolite of $[Al] \leqq 90$.

References and Notes

1 P. Payra, P. K. Dutta, in *Handbook of Zeolite Science and Technology*, ed. by S. M. Auerbach, K. A. Carrado, P. K. Dutta, Marcel Dekker Inc, New York, **2003**, p. 1.
2 A. Corma, in *Fine Chemicals through Heterogeneous Catalysis*, ed. by R. A. Sheldon, H. van Bekkum, Wiley-VCH, Weinheim, **2001**, p. 80.
3 A. Takahashi, R. T. Yang, C. L. Munson, D. Chinn, *Langmuir* **2001**, *17*, 8405.
4 Y. H. Yeom, B. Wen, W. M. H. Sachtler, E. Weitz, *J. Phys. Chem. B* **2004**, *108*, 5386.
5 J. Mon, Y. J. Deng, M. Flury, J. B. Harsh, *Microporous Mesoporous Mater.* **2005**, *86*, 277.
6 C. S. Cundy, P. A. Cox, *Microporous Mesoporous Mater.* **2005**, *82*, 1.
7 Y. Li, R. T. Yang, *J. Phys. Chem. B* **2006**, *110*, 17175.
8 M. Kato, K. Itabashi, A. Matsumoto, K. Tsutsumi, *J. Phys. Chem. B* **2003**, *107*, 1788.
9 W. Loewenstein, *Am. Mineral.* **1954**, *39*, 92.
10 T. Frising, P. Leflaive, *Microporous Mesoporous Mater.* **2008**, *114*, 27.
11 E. Dempsey, G. H. Kühl, D. H. Olson, *J. Phys. Chem.* **1969**, *73*, 387.
12 T. Takaishi, *J. Phys. Chem.* **1995**, *99*, 10982.
13 *Atlas of Zeolite Structure Types*, ed. by W. M. Meier, D. H. Olson, Butterworth-Heinemann, London, **1992**, p. 96.
14 H. Lechert, H. Kacirek, *Zeolites* **1993**, *13*, 192.
15 Supporting Information is available electronically on the CSJ-Journal Web site, http://www.csj.jp/journals/chem-lett/index.html.

